17th World Conference on Earthquake Engineering, 17WCEE
Sendai, Japan - September 13th to 18th 2020

PRELIMINARY STUDY OF SEISMIC PERFORMANCE OF TALL WALLS WITH MINIMUM LONGITUDINAL REINFORCEMENT LIMITS

Tianhua Deng[(1)], Richard S. Henry [(2)]

[(1)] *PhD student, University of Auckland, tden480@aucklanduni.ac.nz*
[(2)] *Senior Lecturer, University of Auckland, rs.henry@auckland.ac.nz*

Abstract

Reinforced concrete (RC) structural walls are effective lateral force-resisting components that are commonly implemented as an RC core wall configuration in tall buildings. Recent studies have investigated the impact of minimum longitudinal reinforcement limits on the ductility of RC walls and resulted in revisions to design standard requirements in both New Zealand and the United States. This prior research focused on rectangular wall sections with a clear plastic hinge region at the wall base, whereas tall buildings tend to use non-rectangular profile and exhibit more distributed plasticity demands up the wall height. In order to investigate the core wall system performance designed in accordance with the current standard, distributed plasticity beam-column fiber element model with a regularisation technique was implemented to simulate the behaviour of the wall piers and concentrated plasticity model was used to simulate the performance of the coupling beams. The modelling technique was validated against four different experimental tests, including the lightly reinforced rectangular wall, C-shaped wall, coupling beam and coupled wall, to ensure each component and the system can be accurately modelled. Following calibration and validation of the models, a push-over analysis will be conducted on a proposed 10-storey tall core wall system satisfying the minimum longitudinal reinforcement requirement over the full wall height to understand the critical section performance where the additional reinforcement in the plastic hinge region terminates.

Keywords: minimum longitudinal reinforcement limit, fiber model, nonrectangular wall, coupling beam, core wall

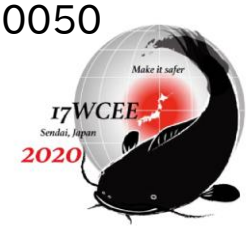

1. Introduction

Reinforced concrete structural walls are commonly selected as the lateral load-resisting component in tall buildings. Coupled core walls systems are the typical configuration, satisfying the requirement for both strength and efficient use of space in architectural design. Recent studies have investigated the impact of minimum longitudinal reinforcement limits on the ductility within the plastic hinge region at the base of rectangular walls. For example, tests of walls with the minimum reinforcement content highlighted the non-ductile and limited ductile response for walls designed in accordance with ACI 318-14 longitudinal reinforcement limits [1]. Alternatively, test walls designed in accordance with revised minimum reinforcement limits in NZS 3101:2006 (A3) indicated that the additional reinforcement at the ends of the wall was capable of generating well-distributed secondary cracks to achieve the targeted ductility [2]. However, tall buildings exhibit more distributed plasticity demand up the wall height because of the higher modes effect [3 4 5]. The termination of longitudinal reinforcement above the well-detailed plastic hinge region at wall base and amplified bending moment lead to the occurrence of the yielding up to the full wall height, where the reinforcement content may not be sufficient to ensure a ductile response is achieved.

In order to extend the previous research into minimum longitudinal reinforcement limits to non-rectangular and tall walls, an investigation of the seismic response of tall RC core wall system with minimum longitudinal reinforcement was conducted. The modelling technique implemented in OpenSees included a displacement-based fiber element model with a regularisation technique for the wall piers and the concentrated plasticity model for the coupling beams. The validation of the model against lightly reinforced rectangular wall tests verified the ability to accurately capture strain localisation and wall failure. The calibration against C-shaped wall, coupling beam and coupled wall system tests ensured the model captured each component and the system behaviour. Following calibration and validation of the models, a push-over analysis will be conducted on a proposed 10-storey tall core wall system satisfying the minimum longitudinal reinforcement requirement over the full wall height.

2. Model description

The model was developed to using efficient approaches to simulate the seismic behaviour of every component in the core wall system. Distributed plasticity beam-column fiber elements have been extensively investigated and applied to simulate the flexural behaviour of RC walls [6 7]. Among a wide variety of fiber models, force-based element (FBE) and displacement-based element (DBE) are the two primary formulations used to simulate the nonlinear response of RC walls. Both of the models permit the plastic hinge forming at any location along with the wall height through the integration of the force-deformation response at sections along the individual element length. The DBE method follows a standard finite element approach where the element deformation equilibrium based upon the interpolation of nodal displacement. In FBE, a linear moment distribution is assumed along with the element that can represent an exact nonlinear response. When a sufficiently refined meshing scheme is used, element number in DBE and integration point number in FBE, both can be successfully used in the nonlinear analysis to achieve comparably response to that of previously test walls. However, in dynamic time-history analysis, DBE performs better convergence characteristics compared to FBE [8]. As a series of time history analysis was planned to conduct in a follow-up study, the DBE was selected for this study.

Regularisation is a fundamental procedure for investigating a mesh objective response in fiber models, because of the characteristic length in the finite element discretisation. Two primary methods were generalised to address the localisation issues in the simulation, including the modification of the material stress-strain properties [9] and the selection of the appropriate integration scheme [10 11].In this study, a thorough method of localisation characteristic for the material properties was developed for the application of nonlinear analysis. For walls designed with the minimum allowable longitudinal reinforcement requirement, the behaviour and failure are controlled by flexural cracking of concrete and fracture of reinforcement (ie. tension controlled). In order to minimise the effect of element length on the strain

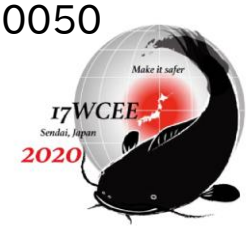

localisation for the lightly reinforced wall, a constant post-yield energy approach was adopted to regularise the reinforcement ultimate strain using the experimental stress-strain energy envelop [12]. Although the strain regularisation defines the reinforcement tension deformation limitation, the ultimate stress affected by the hardening slope is an essential factor to represent the strength capacity within the hardening stage. The integrated application for both strain and developed stress regularisation was proposed to predict the RC components dominated by tension failure. Eq. (1) was proposed for regularising the strain-hardening slope to determine the ultimate stress that based upon the constant energy assumption, where E_s is the initial elastic slope, b is hardening slope coefficient, bE_s is strain-hardening slope, G_s is the post yielding energy, ε_u is ultimate strain, ε_y is the yield strain, and f_y is the yield stress. For the concrete material definition, the low tensile strength and brittle fracture characteristics make the tensile energy difficult to estimate and unlikely to significantly affect the response of failure of RC walls. As such, regularisation for concrete tensile failure was not taken into account in the model developed.

$$bE_s = \frac{2 \times G_s}{L_{IP} \times (\varepsilon_u - \varepsilon_y)} - \frac{2 \times f_y}{(\varepsilon_u - \varepsilon_y)} \tag{1}$$

The fiber element is based upon the Bernoulli-Euler theory that stipulates the plane remain plane section assumption after bending. This assumption states the bending strain maintains evenly distributed across the flange section when subjected to the moment in the direction perpendicular to the flange. Although the fiber element can define the C-shaped wall section consisting of the web and flanges segments as an entire section, the shear lag effect in the core wall configuration violates the plane section assumption [13]. In order to properly predict of the wall strength and minimise the shear lag effect, The C-shaped section was separated into three rectangular regions, i.e., two flanges and one web parts, which were simulated by vertical elements in the centroid of each segment. The proper section of controls the desirable strain localization. The previous study verified four equal-length DBE division for the height of each wall specimen was suitable to perform an acceptable response for the C-shaped section wall [14 15]. Hence, the horizontal rigid link bar connected with each individual web and flange section that was placed at the middle and top of the wall height in each storey.

The fiber element couples the axial and flexural response of the section but ignores the shear response. In order to account shear deformation of the wall elements, the additional zero-length element representing the shear spring was introduced into the model at ¼ and ¾ height of the wall. The equivalent linear elastic shear stiffness was estimated as per Eq. (2), where k_s is the uncracked shear stiffness, G is shear modulus, A_s is 80% of the gross section area and h_l is the tributary length of the shear springs. The constant shear stiffness definition has been shown to be acceptable when compared against the results of C-shaped wall test [14 15].

$$K_s = \frac{GA_s}{h_l} \tag{2}$$

Reinforcement slip and flexural deformations control the response of coupling beams at wall pier interface. The incorporated deformation contributes more than 85% of the total rotation [16]. In order to capture the flexural and slip phenomenon for the diagonal reinforced coupling beam, a combined zero-length element and two node-link element representing the slip spring and flexural rotation spring were introduced into the concentrated plasticity model to simulate the nonlinear response of the coupling beam. The equivalent elastic stiffness for the rigid beam body was estimated as $0.5E_sI_g$, considering the reduced effective stiffness under the in-elastic deformation [17]. It is noted that the parallel incorporation of the slip and flexural rotation spring was adopted for the aggregation of the capacity of springs. The cluster springs setting is dominated by the local reinforcement extension failure since the trigger of the premature slip failure precludes further flexural deformation.

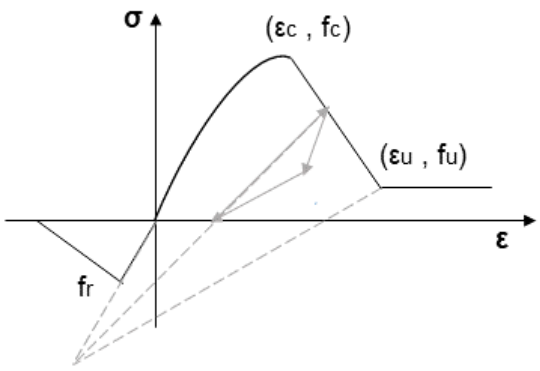

(a)Schematic Concrete02 stress-strain curve

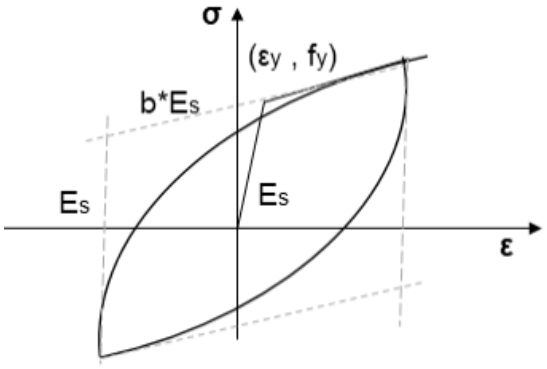

(b)Schematic Steel02 stress-strain curve

Fig.1: Constitutive material models

Uniaxial constitutive material models were used to represent the nonlinear material behaviour within the fiber element sections, and the P-Delta formulation was applied to describe the nonlinear geometric response. A modified Kent-Park concrete model was used to capture the nonlinear behaviour (available in OpenSees as Concrete02) [18]. The Concrete02 is capable of providing a reasonable and comprehensive result that extensively used in RC wall simulation [19 20]. The compressive behaviour of Concrete02 is expressed by three regions, including an ascending parabolic branch, a descending linear branch and a constant residual strength. The tensile behaviour is defined by a bi-linear curve with zero residual strength, as shown in Fig.1 a. The tensile strength was calculated as 0.3 (f_{ck})2/3 in accordance with the fib Model code, where f_{ck} is the characteristic compressive strength [21]. For steel reinforcement, the Giuffré-Menegetto-Pinto hysteretic model in OpenSees defined as Steel02 was selected [22] The Steel02 model describes the stress-strain relation for a linear elastic curve with the slope E_s as the initial elastic modulus. Subsequently, the hardening slope with an introduced coefficient is expressed as bE_s to describe the behaviour after the yielding point, as shown in Fig.1 b. The asymptote for the initial elastic and hardening curve represents the Bauschinger effect during the unload and reload stage. There is no regularisation function built into Steel02, and so the MinMax material command was used to define the tension and compression strain limitation in the stress-strain response. Once the limits were triggered, the reinforcement stress immediately dropped to zero. The material was assigned to the corresponding fibre region according to the actual position in the wall cross-section, and no bond-slip effects were incorporated in the model.

3. Model Comparison and validation

3.1 Wall W1-60-0.14 and W-60-0.24

Wall W1-60-0.14 and W1-60-0.24 were part of the test program to investigate the response of very lightly reinforced concrete walls [1]. The test members were designed with minimum longitudinal reinforcement of 0.15% for the ordinary wall and 0.25% for the special wall in accordance with ACI 318-14 [23].

The model developed was compared against these test results to verify the proposed regularisation method and element number sensitivity for the lightly reinforced concrete walls. Models with the equal length element that consisted of 11, 15 and 19 nodes to exhibit the cracking behaviour for lightly reinforcement test walls. Fig.2 a & b illustrated the partial regularisation that included adjusting only the ultimate strain of the reinforcement material was generally able to capture the wall behaviour but failed to provide an accurate or consistent calculation of ultimate strength. The full regularisation with the incorporated strain and stress regularisation was able to match the experimental result with acceptable accuracy in respect of the cracking strength, ultimate strength and drift capacity at reinforcement fracture, as depicted in Fig.2 c & d. The test and model results both showed the wall specimens displayed a sudden drop in load after the first cracking. For 0.15% reinforcement ratio wall specimen, the ultimate strength was approximately 80% of the strength

prior to cracking with the wall never fully recovering the tensile strength released when the first crack formed. The 0.25% reinforcement ratio specimen dipped temporarily after the first cracking and the ultimate strength prior to reinforcement fracture exceeded the cracking strength. However, the drift ratio of less than 1% indicated the upper wall portion designed with the reinforcement content only likely to achieve a limited ductile response.

There was some discrepancy in the calculated response after cracking with a steeper descending slope calculated by the model compared to the test response. This is due to the rapid strength drop not being able to be recorded with sufficient sampling speed during the testing. In contrast, the recorded response in the numerical model depends on the calculated increment and tolerance for each step, The quantitive data, herein, can be acquired from the modelling result to describe the behaviour after the initial cracking.

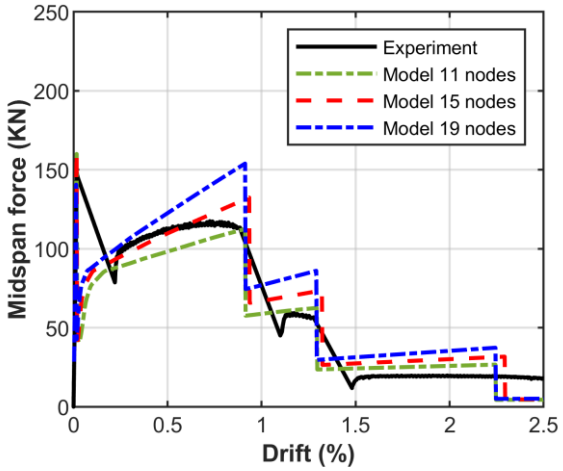

(a) Wall W1-60-0.14 with partial regularisation

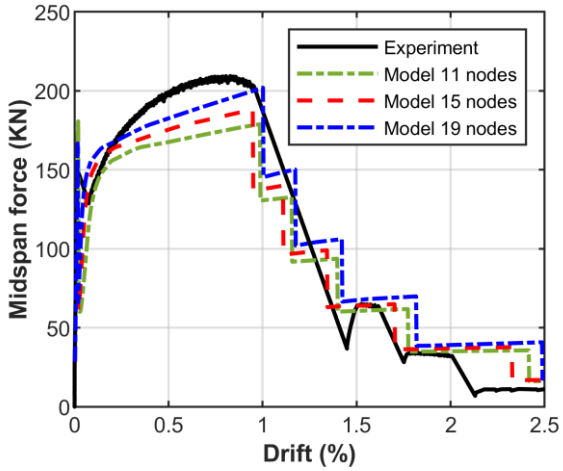

(b) Wall W1-60-0.25 with partial regularisation

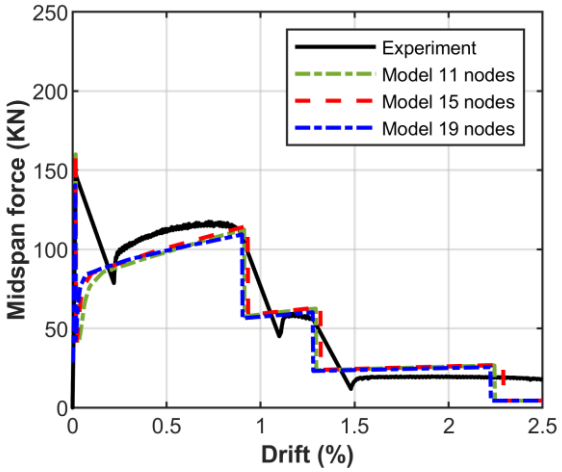

(c) Wall W1-60-0.14 full regularisation

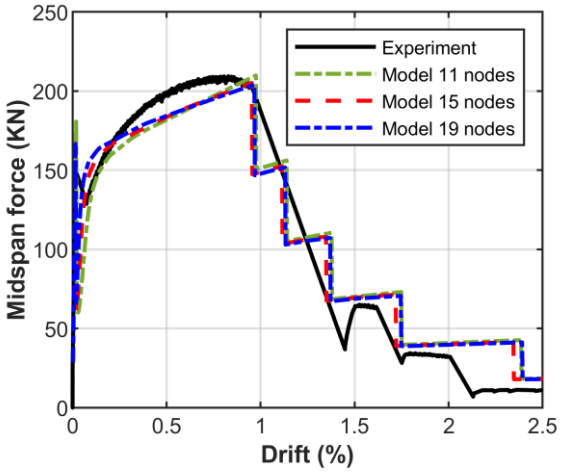

(d) Wall W1-60-0.25 with full regularisation

Fig.2: Comparison of the proposed model with partial and full regularisation technique for tests walls W1-60-0.14 and W1-60-0.24

3.2 C- shaped wall

C-shaped wall TUA was the part of the test program to evaluate the seismic performance of non-rectangular walls [14 24]. The objective of the model was to validate the technique for capturing the global hysteresis behaviour for the C-shaped wall that is representative geometry in the core wall system. Three rectangular

segments were divided to represent the web and flange section. The zero-length elements representing the shear spring was introduced at ¼ and ¾ of wall height and the rigid link bar for section connection was set at the ½ and top of wall height, as discussed in Section 2.

As shown by the comparison in Fig.3, good agreement between the simulated and experimental results was observed. The small discrepancy in stiffness and strength was attributed to the rigid links that did not allow relative deformation at the flange to web connection. Despite this, the walls hysteresis response was still captured with sufficient accuracy by the numerical model.

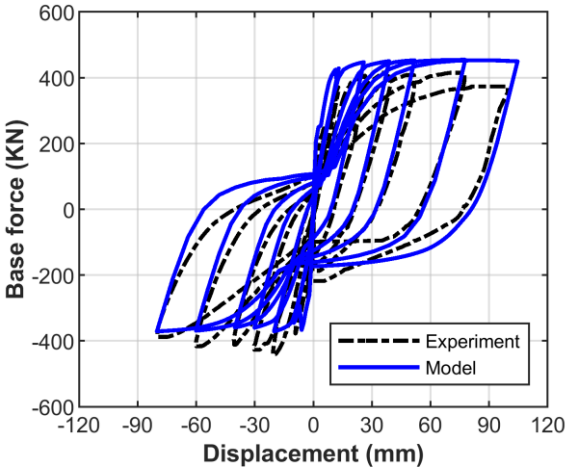

Fig.3: Comparison of the proposed model and the experimental Wall TUA

3.3 Coupling beam

The coupling beam CB-24F was one of the test specimens to investigate the load-deformation behaviour for moderate aspect ratio coupling beams designed with diagonal reinforcement [16 25]. The modelling target was to develop the technique to capture the nonlinear response of the coupling beam, accounting the flexural and slip deformations.

The diagonal reinforcement is regarded as the main contribution for the shear capacity of the coupling beam, with the influence of the confined concrete often ignored [26]. Although this assumption probably underestimates the strength capacity since the well-confined core concrete can also improve the strength, ACI 318-14 presents the formulation to predict the coupling beam strength for conservative propose, as shown in Eq. (3) [23]. Based upon the suggestion of ACI 318-14, the yield strength for the flexural rotation spring was determined by the shear strength V_n multiplied by the span length l_n. The backbone for the acceptance criteria was derived from ASCE 41 to estimate the force-deformation relation [27]. For the definition of the slip spring strength, the extension capacity at cracking was calculated in accordance with recommended formulation for the end-slip yielding reinforcement [28 29].

$$V_n = 2A_{vd} f_y \sin\alpha \tag{3}$$

Compared with the experimental data, the hysteresis behaviour calculated by the model showed good agreement throughout all phases of the response, including as the strength degraded, as depicted in Fig.4. This result confirmed that the incorporation of slip and flexural springs scheme was suitable to predict the response of coupling beams.

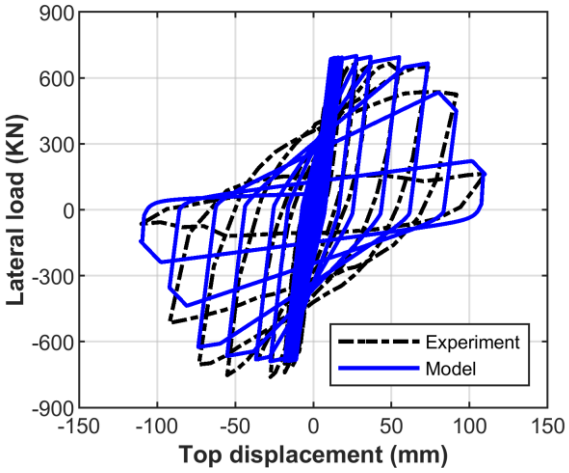

Fig.4: Comparison of the proposed model and experimental Coupling Beam CB24F

3.4 Coupled wall

The coupled wall CW1 was tested to investigate the seismic response for a 10-storey planar coupled wall, where the lower 3 stories of the prototype wall were tested in the laboratory [30 31]. A comprehensive loading prototype combined with the lateral force and moment was applied on the individual wall pier to simulate the real force situation in the full 10-storey wall. In order to simplify the loading protocol for modelling, the entire 10-storey height wall was constructed in the model with the apportionment of inverted triangle lateral loading at each storey up the full wall height. The performance of the lower three stories was recorded and compared against the test wall response, as shown in Fig.5.

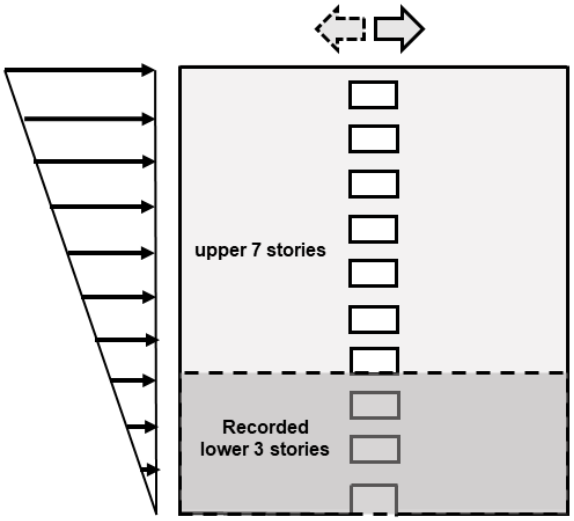

Fig.5: Schematic illustration of the loading protocol

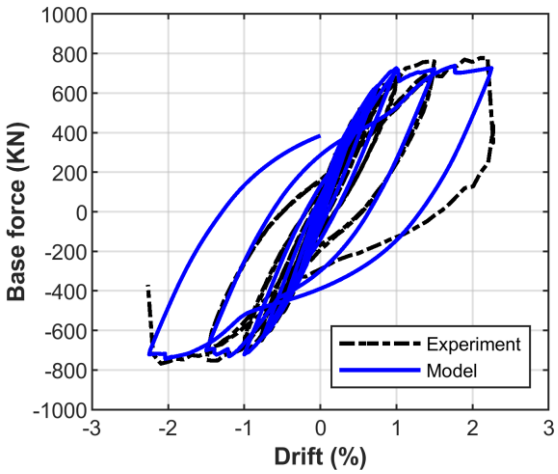

Fig.6: Comparison of the proposed model and experimental Coupled Wall CW1

The objective of the simulation was to validate the response of the coupled wall by means of the synthesis of the wall and coupling beam modelling techniques. As shown by the comparison in Fig.6, good agreement between the simulated and experimental results was observed. It was concluded that the proposed model technique for the wall piers and coupling beam was suitable to predict the response of the entire core wall system.

4. Future work

Based on the calibrated models presented in the previous section, the fiber element with shear spring model formulation will be used to investigate the lateral load response of a 10-storey core wall system designed in accordance with ACI 318-19. The core wall geometry was selected from an existing 10-storey model that consisted of two 210 mm thick C-shaped wall with a 2.3 m length flange and 4.6 m length web [5]. Each storey was 3.5 m high with a total wall height was 35 m. The dimensions of the coupling beam were 210 mm wide, 600 mm high and 1.2 m clear span. The wall was designed with a specified concrete strength of 43 MPa and calculated tensile strength of 3.6 MPa. The properties of Grade 60 reinforcement were 480 MPa yield strength and 730 MPa ultimate strength, as recommended by tall building design guidelines [32]. ACI 318-19 includes new minimum longitudinal reinforcement provisions that require additional longitudinal reinforcement extending from the critical section distance not less than the greater of l_w and $M_u/3V_u$, where l_w is the wall length and M_u/V_u is the factored shear span ratio. In order to investigate the impact of terminating additional longitudinal reinforcement on the flexural demand, the 10-storey core wall was designed with the minimum longitudinal reinforcement contents required by ACI 318-19 and comparing the termination length of $M_u/4V_u$ (2 storeys), $M_u/3V_u$ (3 storeys), $M_u/2V_u$ (4 storeys) and full height (10 storeys).

For the wall section in the plastic hinge region, the minimum end zone longitudinal reinforcement ratio of 0.68% $(\sqrt{f_c'}/2f_y)$ was required leading to 11 × #4 (D12.7) bars (diameter = 12.7 mm) placed at web and flange corners to achieve a reinforcement ratio of 0.74%, and 5 × #4 (D12.7) bars (diameter = 12.7 mm) placed at end of flange to achieve a reinforcement ratio of 0.75%. The distributed minimum longitudinal reinforcement ratio of 0.25% was required in the wall web region, resulting in two layers of 12 × #3 (D9.5) bars (diameter = 9.5 mm) placed at 250 mm centres over the wall length, as shown in Fig.7a. For the wall section outside the plastic hinge region, the distributed minimum longitudinal reinforcement ratio of 0.25% was required for the entire wall section, resulting in two layers of #3 (D9.5) bars (diameter = 9.5 mm) placed at 250 mm centring over the web and flange length, as shown in Fig.7b. The imposed axial load was assumed as 0.3% f_c' A_g for each storey leading to 3% f_c' A_g acting at the total base. The core wall will be loaded in the web direction, using an inverted triangular lateral load pattern up the entire wall height, as depicted in Fig.8.

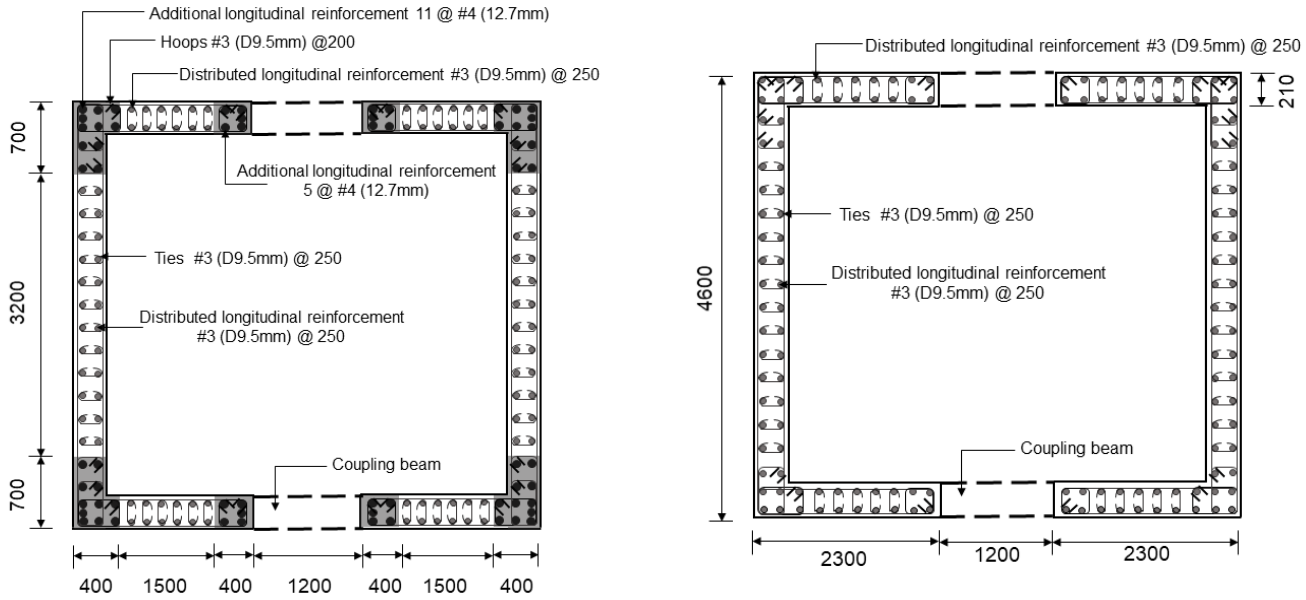

(a) Wall base - plastic hinge region (b) Outside of the plastic hinge region

Fig.7: Section details for the core wall

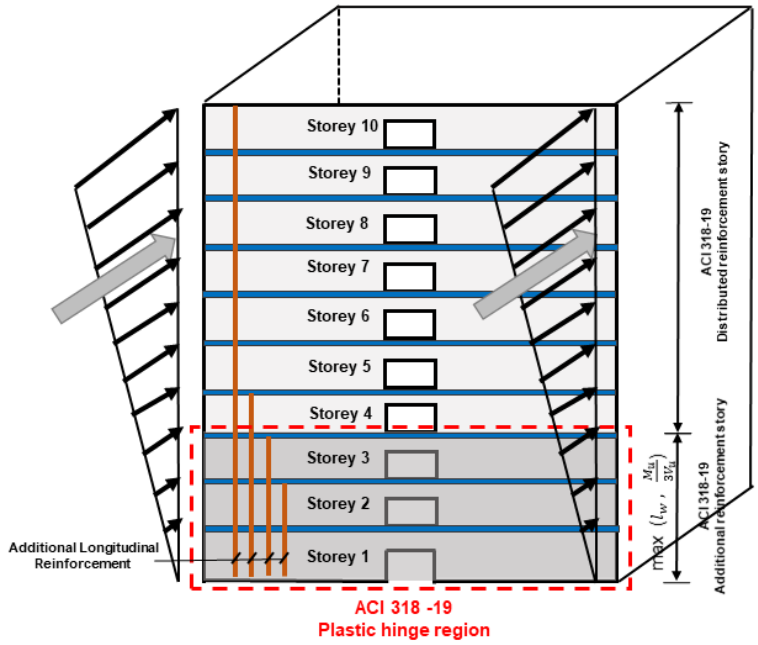

Fig.8: Loading protocol for a 10-storey core wall designed by ACI 318-19

4. Summary

The current requirements for minimum longitudinal reinforcement in ductile walls were developed for the plastic hinge region and the effect of reduced longitudinal reinforcement in the upper section of tall walls have not been thoroughly investigated. An efficient modelling technique had been developed for the core walls and calibrated against the experimental tests from the lightly reinforced walls, nonrectangular walls, coupling beams, and coupled wall systems. Modelling of a 10-storey core wall system designed in accordance with ACI 318-19 minimum reinforcement requirement is ongoing to investigate the impact of terminating additional longitudinal reinforcement on the lateral load response. According to the presented numerical analysis, the following preliminary conclusions can be drawn:

- For the walls designed with the minimum longitudinal reinforcement requirement, both ultimate strain and strain hardening slope regularisation of reinforcement properties are essential to capture the behaviour of lightly reinforced walls controlled by tension failure.
- The concentrated plasticity model with the slip and flexural rotation springs can capture the response of coupling beams throughout all phase of their response.
- The four equal-length DBE divisions with the combination of shear springs and rigid link bars can provide a relatively accurate simulation of non-rectangular walls.

5. Acknowledgements

The authors wish to acknowledge the Chinese Scholarship Council and the University of Auckland to provide financial support for this research program. In addition, the authors are grateful for the contribution of Dr. Ash. Puranam, Prof. Katrin. Beyer, Assistant Prof. David Naish and Prof. Dawn. Lehman for kindly sharing the experimental data.

Reference

[1] Puranam, A., & Pujol, S. (2017). Minimum Flexural Reinforcement in Reinforced Concrete Walls. *16th World Conference on Earthquake, 16WCEE 2017*, 1–10.

[2] Lu, Y., Gultom, R., Henry, R. S., & Ma, Q. T. (2016). Testing of RC walls to investigate proposed minimum vertical reinforcement limits in NZS 3101 : 2006 (A3), *2006*(2015), 1–8.

[3] Blakeley.R.W.G., R.C.Cooney., & L.M.Negget. (1975). Seismic Shear Loading At Flexural Capacity in Cantilever Wall Structures. *Bulletin of the New Zealand National Society for Earthquake Engineering*, *8*(December).

[4] Priestley, M. J. N., Calvi, G. M., & Kowalsky.M.J; (2007). *Displacement-Based Seismic Design of Structures*. IUSS Press.

[5] Panagiotou, M., & Restrepo, J. I. (2009). Dual-plastic hinge design concept for reducing higher-mode effects on high-rise cantilever wall buildings. *Earthquake Engineering & Structural Dynamics*, *37*, 1359–1380.

[6] Spacone., E., Filippou., F. C., & Taucer, F. F. (1996). Fibre Beam-Column Model for Non-Linear Analysis of R/C Frames: Part I. Formulation. *Earthquake Engineering & Structural Dynamics*, *25*(7), 711–725.

[7] Pugh, J. S. (2012). *Numerical Simulation of Walls and Seismic Design Recommendations for Walled Buildings*. University of Washington.

[8] Marafi, N. A., Ahmed, K. A., Lehman, D. E., & Lowes, L. N. (2019). Variability in Seismic Collapse Probabilities of Solid- and Coupled-Wall Buildings. *Journal of Structural Engineering*, *145*(6), 04019047.

[9] Coleman.J & Spacone.Enrico. (2001). Localization Issues in Force-Based Frame Elements. *Journal of Structural Engineering*, *127*(November), 1257–1265.

[10] Scott, M. H & Fenves, G. L. (2006). Plastic Hinge Integration Methods for Force-Based Beam–Column Elements. *Journal of Structural Engineering*, *132*(2), 244–252.

[11] Scott, M. H & Ryan, K. L. (2013). Moment-rotation behavior of force-based plastic hinge elements. *Earthquake Spectra*.

[12] Pugh, J. S. (2012). *Numerical Simulation of Walls and Seismic Design Recommendations for Walled Buildings*. *PhD Thesis, University of Washington*. University of Washington.

[13] Kwan, A. K. H. (2002). Shear Lag in Shear/Core Walls. *Journal of Structural Engineering*, *122*(9), 1097–1104.

[14] Beyer, K. (2007). *Seismic design of torsionally eccentric buildings with U-shaped RC Walls*. Rose School.

[15] Arabzadeh, H & Galal, K. (2018). Seismic-Response Analysis of RC C-Shaped Core Walls Subjected to Combined Flexure, Shear, and Torsion. *Journal of Structural Engineering*, *144*(10),

[16] Naish, D., Fry, A., Klemencic, R., & Wallace, J. (2013). Reinforced Concrete Coupling Beams — Part II : Modeling. *ACI Structural Journal*, *110*(6), 1067–1075. http://nees.org/warehouse/project/1100

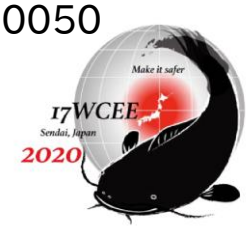

[17] FEMA 356. (2000). *Prestandard and Commentary for the Seismic Rehabilitation of Building*. *Federal Emergency Management Agency*.

[18] Yassin Mohd, M. H. (1994). *Nonlinear analysis of prestressed concrete structures under monotonic and cyclic loads*. University of California, Berkeley.

[19] Orakcal, K., Massone, L. M & Wallace, J. W. (2006). Analytical modeling of reinforced concrete walls for predicting flexural and coupled-shear-flexural responses. *Pacific Earthquake Engineering Research (PEER) Center*, (October), 228.

[20] Encina, E & Henry, R. (2015). Preliminary investigation of elongation in RC walls. In *2015 NZSEE Conference*.

[21] fib Bulletin 65. (2012). *fib Model Code 2010 Volume 1*. *the International Federation for Structural Concrete (fib)*.

[22] Filippou.F.C., Popov.E.P & Beryero.V.V. (1983). *Effects of Bond Deterioration on Hysteretic Behavior of Reinforced Concrete Joints*. Earthquake Engineering Research Center, University of California,.

[23] ACI Committee 318. (2014). *Building Code Requirements for Structural Concrete(ACI 318-14)* (Vol. 11).

[24] Experimental data resource. https://zenodo.org/record/21846#.XkTQImgzY-V;

[25] Experimental data resource. http://nees.org/ warehouse/project/1100

[26] Paulay, T & Binney, J. R. (1974). Diagonally reinforced coupling beams of shear walls. *American Concrete Institute Structural Journal, SP-42*(2), 579–598.

[27] ASCE 41-06. (2007). *Seismic Rehabilitation of Existing Buildings*. American Society of Civil Engineers.

[28] Alsiwat, B. J. M & Saatcioglu, M. (1992). Reinforcement Anchorage Slip under Monotonic Loading. *Journal of Structural Engineering*, *118*(9), 2421–2438.

[29] Zhao, J & Sritharan, S. (2007). Modeling of Strain Penetration Effects in Fiber-Based Analysis of Reinforced Concrete Structures. *ACI Structural Journal*, (104), 133–142.

[30] Lehman, D. E., Turgeon, J. A., Birely, A. C., Hart, C. R., Marley, K. P., Kuchma, D. A., & Lowes, L. N. (2013). Seismic Behavior of a Modern Concrete Coupled Wall. *Journal of Structural Engineering*, *139*(8), 1371–1381.

[31] Experimental data resource. http:// nees.org/warehouse/project/104

[32] Los Angeles Tall Buildings Structural Design Council. (2017). *An Alternative Procedure for Seismic Analysis and Design of Tall Buildings Located in the Los Angeles Region*.

